

# MICRO-CT SYSTEM FOR SMALL ANIMAL IMAGING WITH ULTRAFAST LASER-BASED X-RAY SOURCE

*A. Krol<sup>1</sup>, J-C. Kieffer<sup>2</sup>, L. Chen<sup>2</sup>, R. Toth<sup>2</sup>, I. L. Coman<sup>3</sup>, E. D. Lipson<sup>4</sup>, R. E. Kincaid<sup>4</sup>, and Charles C. Chamberlain<sup>1</sup>*

<sup>1</sup>Department of Radiology, SUNY Upstate Medical University, USA

<sup>2</sup>INRS-Énergie et Matériaux, Université du Québec, Canada

<sup>3</sup>Department of Computer Science and Mathematics, Ithaca College, Ithaca, NY, USA

<sup>4</sup>Department of Physics, Syracuse University, Syracuse, NY, USA

## ABSTRACT

A novel ultrafast-laser-based x-ray source is a promising candidate for replacement of a microfocal X-ray tube in a micro-CT system for small-animal imaging. We optimized conditions for x-ray generation from a very small (below 5  $\mu\text{m}$ ) focal spot. We measured x-ray spectra, conversion efficiency, x-ray fluence, and x-ray focal-spot size for a number of solid targets ( $\text{SiO}_2$ , Ge, Mo, Ag, Sn,  $\text{BaF}_2$ , La, Nd, Gd, Ta, and Pb). X-ray spectra created by ultrafast laser are advantageous for micro-CT imaging, because most of the emission is in narrow characteristic lines. The spectra can be changed rapidly and matched to the imaging task. They make practical the use of dual-energy micro-CT with suitable contrast agents and matching targets and filters for low- and high-energy beams. We have obtained images of small animals in single- and dual-energy modes.

## 1. INTRODUCTION

The tomographic images created by micro-CT for small-animal imaging are only as good as the projection images obtained using the microfocal x-ray tube. However, a conventional x-ray source suffers from severe limitations, including the limited maximum power (typically below 10 W for 5  $\mu\text{m}$  focal spot) [1,2] and, for most applications, suboptimal spectral shape of x-ray spectra, because the useful anode materials are limited to a few metals (Cu, Mo, and W) and the anode-cathode voltage differential has to be relatively large (typically over 40 kVp). A novel, ultrafast laser-based x-ray (ULX) source replacing the microfocal tube might alleviate these limitations and provide an enhanced tool for small-animal imaging. ULX could shorten scan time, because the average power of ULX exceeds the maximum power of a microfocal x-ray tube. It could ensure better dose

utilization and limit the beam-hardening effect, because it generates narrow x-ray emission lines that can be easily tuned to the imaged animal size and density. In addition, ULX could be useful in dual energy micro-CT for small-animal imaging with suitable contrast agent (containing I, Ba, Gd, etc.). This could be achieved by using selected laser targets and matching filters for low- and high-energy beams that would bracket the K-edge of interest.

## 2. X-RAY GENERATION BY ULTRAFAST LASERS

Ultrafast lasers were invented in the mid 1980's [3]. Presently, tabletop, terawatt ultrafast-lasers produce pulses with femtosecond duration. As a result, extremely high optical power density ( $10^{18}$ – $10^{20}$   $\text{W}/\text{cm}^2$ ) can be delivered to a spot on the target with diameter  $\sim 5$   $\mu\text{m}$  or smaller. The peak electric field of such an intense beam exceeds  $10^{11}$  V/m.

When the laser-light power surface density on the solid target exceeds  $\sim 5 \times 10^{12}$   $\text{W}/\text{cm}^2$ , a very thin layer of inhomogeneous, cold, and dense plasma is formed. Up to 40% of the laser energy can be transferred from laser light to suprathermal (hot) electrons through resonance absorption, vacuum heating, JxB heating, and other effects [4]. Many of the hot electrons are released from the dense-plasma region creating a charge "cloud" above the target and leaving behind an intense positive space-charge field. It attracts the energetic hot electrons, which return and penetrate the target. This results in a short lasting burst of incoherent x-rays that consist of continuous bremsstrahlung and characteristic emission lines. The continuous emission can span from several tens of keV to a few MeV, depending on the parameters of the laser and the plasma, whereas the emission lines are in the range of 1–100 keV depending on the atomic number of the target material. The x-ray pulse lasts longer than the laser pulse, generally ranging from several hundreds of femtoseconds to several picoseconds. The x-ray source size is larger than

the laser spot size. Examples of ULX spectra that might be useful for rodent imaging are shown in Figs. 1–2.

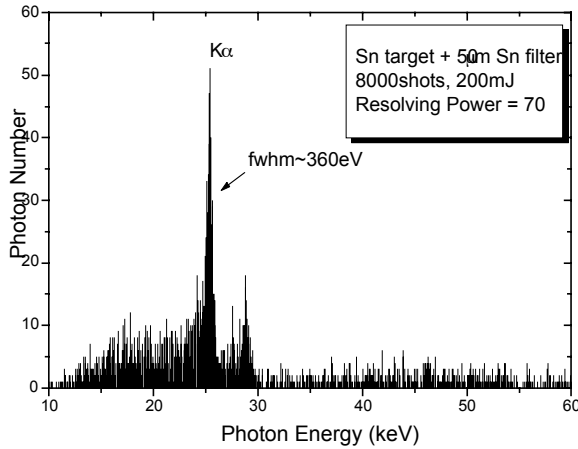


Fig. 1. X-ray spectrum obtained for Sn target and Sn filter with INRS 10 Hz ultrafast laser).

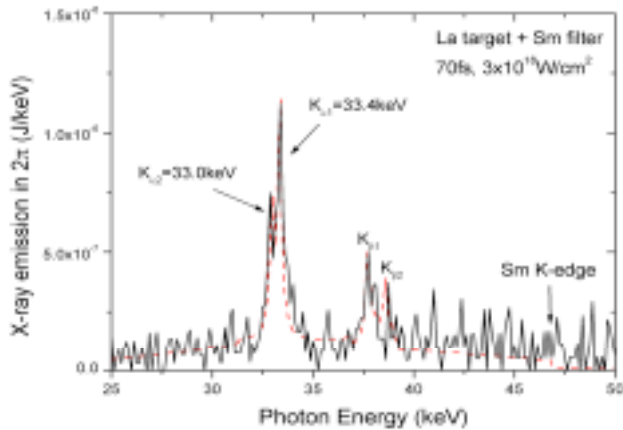


Fig. 2. Fig. 1. X-ray spectrum obtained for La target and Sm filter with INRS 10 Hz ultrafast laser). Solid line: experiment. Dashed line: fit (bremsstrahlung + K-lines + Sm filter).

The ultrafast laser pulse ablates a small crater (5  $\mu\text{m}$  diameter and 2  $\mu\text{m}$  in depth) on the target surface, and fresh target surface is exposed to each laser shot (via a precision target-positioning system). There are two major advantages of this technique: i) there is no need to prevent the target from melting and therefore there is no upper limit on the laser power that can be delivered to the target, and ii) the targets with different elemental composition can be irradiated in very short succession, thus allowing for rapid change of x-ray spectra. We note that a current state-of-the-art ultrafast laser can deliver up to 50 W power to a focal spot smaller than 4  $\mu\text{m}$ . The relationship between the power emitted in x-rays and the average ultrafast laser power is shown in Fig. 3.

Fig. 3. Power emitted in x-ray vs. average ultrafast laser power for various optical power density on the target. The 10 Hz laser presently used for imaging at the INRS is shown, as well as an Advanced Laser Light Source (ALLS) laser that will be commissioned in late 2004.

We measured x-ray spot sizes (using knife-edge method) for a number of solid targets (including  $\text{SiO}_2$ , Ge, Mo, Ag, Sn,  $\text{BaF}_2$ , La, Nd, Gd, Ta, and Pb). We observed that the x-ray spots are approximately elliptical in shape (2–5  $\mu\text{m} \times 4$ –15  $\mu\text{m}$ ) with the longer axis oriented parallel to the plane of the light incidence. The actual size depends strongly on the laser-beam focusing and on the pulse duration. A focal spot as small as 1.6  $\mu\text{m}$  can be achieved if a deformable mirror is used [5].

### 3. ENERGY OPTIMIZATION FOR MICRO-CT

Because the laser target elemental composition can be changed rapidly, ULX is well suited for energy optimization in micro-CT of small animals. For example, a Mo target will produce lines around 17 keV, while a Sn target will produce lines around 25 keV. It has been shown that, in order to achieve optimal contrast resolution with a minimum number of photons, for single energy imaging, the average total linear absorption coefficient of the sample,  $\mu(E)$ , has to match the characteristic dimension of the sample ( $D$ ), i.e.  $\mu(E) \approx 2/D$  [2,6].

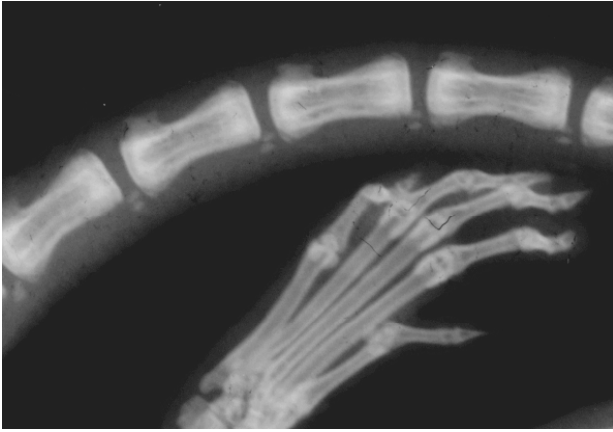
Depending on small-animal composition, the optimal energy lies in the 10–35 keV range, for  $D$  in the 5–15 mm range. The optimal contrast resolution at minimum dose might result in a different optimal energy depending on the targeted-organ dose location [7]. One should expect the dose savings while using ULX, because of better matching of the narrow x-ray emission lines to the animal thickness and density, as compared to the broad spectra produced by x-ray tubes.

K-edge subtraction micro-CT with a contrast agent (containing I, Ba, Gd, etc.) could be practically implemented with ULX. This technique requires an energy difference as small as possible between high- and low-energy beams that have to bracket the absorption line of the contrast agent. While this is difficult with a conventional microfocal x-ray tube, it is quite practical with ULX. For example, for a contrast agent with Barium (K-edge at 37.42 keV), suitable targets include Nd (emission lines at 37.36 and 36.85 keV) for the low-energy beam, and Gd (emission lines at 43.0 and 43.3 keV) for the high-energy beam.

### 4. SMALL-ANIMAL IMAGES OBTAINED WITH ULX

An example of a small-animal image obtained with ULX in a single-energy mode is shown in Fig. 4.

Fig. 4. Distal hind limb and tail of a rat ~10 weeks old; 10 Hz laser at



INRS; Mo target; Mo filter; SOD = 15.0 cm; SID = 30.0 cm; pulse duration: 60 fs; energy per pulse: 300 mJ; p-polarization; contrast:  $10^{-6}$ ;  $\lambda = 400$  nm; hot electron temperature: 20 keV; repetition rate: 10Hz; Fuji EC-MA cassette/AD film used as an image detector.

An example of a K-edge subtraction image of a small animal obtained with ULX in a dual energy mode is shown in Fig. 5.

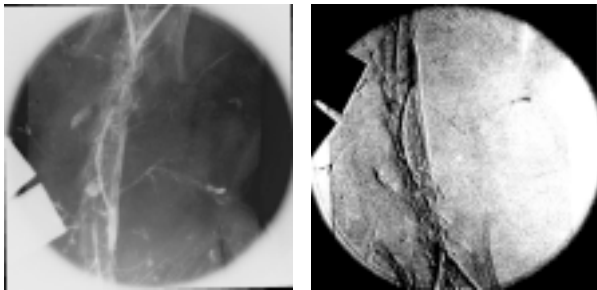


Fig. 5. Left: image of a rat's vasculature containing Ba contrast agent obtained using ULX 10 Hz laser at INRS with Nd target and Nd filter. Right: differential Gd-Nd image of the same rat obtained after subtraction, from the image on the left, of a ULX image obtained with Gd target and Nd filter. Laser parameters were the same as in Fig. 3.

## 5. DESIGN OF MICRO-CT SYSTEM WITH ULTRAFAST LASER-BASED X-RAY SOURCE

A block diagram of a proposed ultrafast-laser-based microtomography system is shown in Fig. 6. The system is very similar to a conventional one, but with the microfocus tube substituted by an ultrafast laser optically coupled to a laser target chamber. As mentioned above, the target transport system must be very accurate, and must position the fresh target surface with  $1 \mu\text{m}$  accuracy for each successive laser shot. For this purpose a precise feedback system needs to be developed and implemented for beam positioning and target rastering. Laser-beam

focusing within the diffraction limit ( $\sim 1.5 \mu\text{m}$ ) will be accomplished by adaptive optics to correct for the laser wave-front distortion and to pre-compensate for the aberrations caused by the focusing optics.

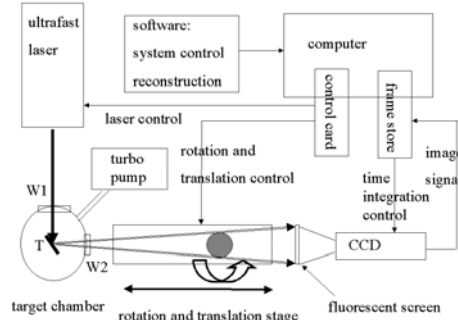


Fig. 6. Simplified block diagram of proposed ultrafast-laser-based micro-CT system for small-animal imaging.

The system specifications are:

- selectable scan time (depending on required resolution), typically 5 times shorter than comparable conventional micro-CT scan
- 3D field of view:  $30 \times 30 \times 30 \text{ mm}^3$
- specimen size up to 30 mm diameter and 120 mm long (in 4 bed positions)
- selectable spatial resolution:  $4\text{--}50 \mu\text{m}$  (depending on dose limitation)
- cone-beam acquisition geometry
- CCD detector with x-ray converter screen optimized for the specific target(s) ULX

We plan to investigate, in collaboration with Radiation Monitoring Devices, Inc., application of microcolumnar CsI(Tl) films on various substrates that will maximize spatial resolution and light output, while minimizing the associated noise for ULX. The CsI(Tl) vapor-deposition protocols to manufacture  $10\text{--}180 \mu\text{m}$  thick films required for  $10\text{--}50 \text{ keV}$  x-ray detection will be modified during this development. The specific goal will be develop screens that will maximize spatial resolution and light output, while minimizing the associated noise.

We plan to develop new imaging protocols to take full advantage of the flexible x-ray spectra provided by ULX in single and multiple energy modes.

## 6. CONCLUSIONS

Our initial studies on application of ULX as a replacement for a microfocus x-ray tube in a small animal micro-CT system indicate that a novel x-ray source might yield the following advantages: shorter scan duration, lower radiation dose, and limited beam-hardening artifact. Further, it might allow practical implementation of dual-energy micro-CT via K-edge subtraction with a suitable contrast agent for enhanced contrast resolution.

## 7. REFERENCES

- [1] M.J. Flynn, S.M. Hames, D.A. Reiman, and S.J. Wilderman, "Microfocused x-ray source for 3-D microtomography," *Nuc. Instrum Methods Phys Res. Sect A* vol. 353, pp. 312-315, 1994.
- [2] M. J. Paulus, et al "High resolution x-ray computed tomography," *Neoplasia*, vol 2, pp. 62-70, 2000.
- [3] D. Strickland and G. Mourou "Compression of amplified chirped optical pulse." *Opt. Commun*, vol. 56, pp. 219, 1985.
- [4] J. C. Kieffer, Z. Jiang, A. Ikhlef, C. Y. Cote, and O. Peyrusse, "Picosecond dynamics of a hot solid-density plasma," *J.Opt. Soc. Am.* vol. B13(1), pp.132-137 (1996).
- [5] O. Albert et al., *Opt. Lett.*, vol. 25, pp. 1125, 2000.
- [6] L. Grodzins, "Optimum energies for x-ray transmission tomography of small samples," *Nucl. Instr. Methods*, vol 206, pp. 541-545, 1983.
- [7] P. Spanne P, "X-ray energy optimization in computed tomography," *Phys. Med. Biol.* Vol. 34, pp. 679-690, 1989.